Direct Measurement of Angles Between Bond Vectors in High-Resolution NMR

Bernd Reif, Mirko Hennig, Christian Griesinger*

Angles between two interatomic vectors are measured for structure elucidation in solution nuclear magnetic resonance (NMR). The angles can be determined directly by using the effects of dipole-dipole cross-correlated relaxation of double-quantum and zero-quantum coherences. The measured rates can be directly related to the angular geometry without need for calibration of a Karplus-type curve, as is the case for scalar coupling measurements, and depend only on the rotational correlation time of the molecule as an empirical parameter. This makes the determination of torsional angles independent from the measurement of coupling constants. The two interatomic vectors can in principle be arbitrarily far apart. The method was demonstrated on the measurement of the peptide backbone angle ψ in the protein rhodniin, which is difficult to determine in solution by NMR spectroscopy.

Structure determination of biomolecules by NMR spectroscopy in solution relies on the measurement of interatomic distances (*1*) that are accessible by the nuclear Overhauser effect (NOE) (*2*) induced by the dipolar coupling between proton nuclei and the determination of torsional angles that can be derived from scalar coupling constants once an empirical correlation, the Karplus relation, of the measured scalar couplings with determined torsional angles (*3*) has been established. The accessibility of this information has grown rapidly over the last years by the introduction of multidimensional NMR spectroscopy (*4*) and the availability of uniformly ^{13}C- and ^{15}N-labeled biomacromolecules (*5*). Nevertheless, the current limitations on structure determination are twofold: NOE intensities fall off rapidly as the distance between the protons involved increases, and coupling constant information relies on calibration of Karplus relations.

Here, we introduce a method to determine the angles between two vectors connecting two pairs of nuclei within a molecule by solution NMR (Fig. 1). No empirical calibration is required to determine the included angle. The method relies on relaxation via cross-correlated dipolar couplings between the four nuclei that form the two internuclear vectors under consideration. Cross-correlated relaxation has so far been considered to be a cumbersome disturbance to high resolution spectra. It has been used only rarely to derive structural information (*6*). In solid-state NMR spectroscopy, the use of dipolar couplings to determine intertensorial angles is widely used (*7*) and has been recently extended to biomolecules in the solid state (*8*, *9*).

Dipolar couplings which constitute the through space magnetic interaction between two nuclei are averaged out in solution due to the isotropic tumbling of biomolecules. However, dipolar couplings are an effective source of relaxation of spin coherences (*10*) due to the stochastic modulation of the local fields according to the angular diffusion of the whole molecule in solution with a time constant in the ps to ns range. The efficiency of the relaxation depends on the time correlation of the dipolar coupling with itself (autocorrelation) or with another dipolar coupling (cross-correlation) (*11*). Without loss of generality, we discuss in the following a carbon-proton and a nitrogen-proton spin pair. Double-quantum coherence involving the nitrogen and carbon transitions can be excited and indirectly detected, which yields a four-line spectrum whose line splittings are the scalar couplings between H^N and N as well as H^C and C (Fig. 2). The relaxation rates $\Gamma_{\mu\nu}$ for the four transitions that are reflected in the line widths are given by the following equations (*12*)

$$\begin{aligned}
\Gamma_{\alpha\beta} &= \Gamma^a - \Gamma_i^{CSA/DD} + \Gamma_j^{CSA/DD} - \Gamma_{i,j}^c \\
\Gamma_{\alpha\alpha} &= \Gamma^a + \Gamma_i^{CSA/DD} + \Gamma_j^{CSA/DD} + \Gamma_{i,j}^c \\
\Gamma_{\beta\beta} &= \Gamma^a - \Gamma_i^{CSA/DD} - \Gamma_j^{CSA/DD} + \Gamma_{i,j}^c \\
\Gamma_{\beta\alpha} &= \Gamma^a + \Gamma_i^{CSA/DD} - \Gamma_j^{CSA/DD} - \Gamma_{i,j}^c
\end{aligned} \tag{1}$$

The indices i and j denote in this case the $N\text{-}H_i^N$ and the $C\text{-}H_j^C$ vector, respectively. The term Γ^a defines the contributions due to autocorrelated relaxation for the individual spectral lines. $\Gamma_{i/j}^{CSA/DD}$ describe the sum of all interactions due to dipole-CSA cross-correlated relaxation for the $N\text{-}H_i^N$ and the $C\text{-}H_j^C$ vector, respectively. CSA is chemical shift anistropy and refers to the orientation dependence of chemical shifts. $\Gamma_{i,j}^c$ is the desired contribution resulting from dipole-dipole cross-correlated relaxation.

These relaxation rates can be determined from the intensities of the corresponding resonance lines in a constant-time NMR experiment, in which the intensity $I_{\mu\nu}$ of a resonance line has decayed by $\exp(-\Gamma_{\mu,\nu}T)$ after a given time T. Except for the overall relaxation Γ^a which does not yield any structural information all other relaxation rates can be determined according to the equations

$$\begin{aligned}
\Gamma_{i,j}^c &= \frac{1}{4T} * \ln\left(\frac{I(\alpha\beta) * I(\beta\alpha)}{I(\alpha\alpha) * I(\beta\beta)}\right) \\
\Gamma_i^{CSA/DD} &= \frac{1}{4T} * \ln\left(\frac{I(\alpha\beta) * I(\beta\beta)}{I(\alpha\alpha) * I(\beta\alpha)}\right) \\
\Gamma_j^{CSA/DD} &= \frac{1}{4T} * \ln\left(\frac{I(\beta\beta) * I(\beta\alpha)}{I(\alpha\alpha) * I(\alpha\beta)}\right)
\end{aligned} \tag{2}$$

where T is the delay in the experiment during which double-quantum coherence evolves. $I(\alpha\alpha)$, $I(\alpha\beta)$, $I(\beta\alpha)$, and $I(\beta\beta)$ are the intensities of the corresponding resonance lines in the spectrum. For a macromolecule that tumbles slowly in solution, the cross-correlated dipolar relaxation depends on the angle θ between the $C\text{-}H_j^C$ and $N\text{-}H_i^N$ bonds (*11*, *13*) according to

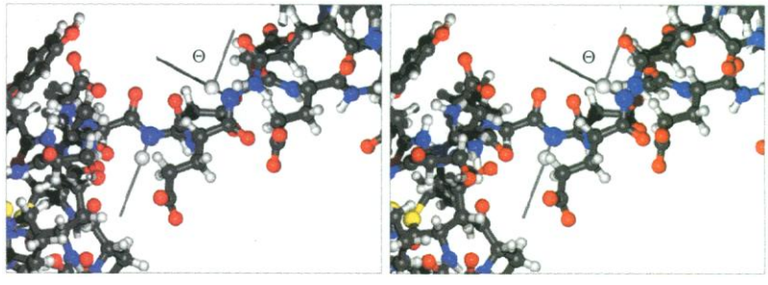

Fig. 1. Stereoview showing a close-up of the structure of rhodniin. The two gray lines indicate the bond vectors of two spin pairs. The angle between the two interatomic vectors is indicated by θ. Atoms are depicted by the following colors: hydrogen, white; carbon, black; sulfur, yellow; oxygen, red; and nitrogen, blue.

Institut für Organische Chemie, Marie-Curie-Straße 11, Universität Frankfurt, D-60439 Frankfurt, Germany.

*To whom correspondence should be addressed. E-mail: cigr@krypton.org.chemie.uni-frankfurt.de

$$\Gamma^{c}_{i,j} = \frac{\gamma_H\gamma_N}{(r_{N,H_i})^3}\frac{\gamma_H\gamma_C}{(r_{C,H_j})^3}\left(\frac{\hbar\mu_0}{4\pi}\right)^2 \times \frac{2}{5}(3\cos^2\theta - 1)*\tau_c \quad (3)$$

The gyromagnetic ratios γ_H, γ_N, and γ_C are nuclear properties, the one-bond distances are normally known from x-ray or neutron diffraction studies and the other constants are natural constants. The correlation time of the molecule τ_c can be determined from relaxation measurements (*14*). Equation 3 does not take fast internal motion and anisotropic reorientation of the molecule into account. These parameters can be measured from independent experimental methodology (*15*) and used for the analysis of the cross-correlated relaxation rates.

We concentrate from now on the measurement of the angle θ between the $C_{\alpha,k}$–$H_{\alpha,k}$ bond vector contained in one amino acid residue and the N_{k+1}-H^N_{k+1} bond vector contained in the following amino acid residue in a protein (Fig. 3). The angle θ depends only on the torsional angle ψ according to the equation: $\cos\theta = 0.163 + 0.819\cos(\psi - 119°)$, assuming the planarity of the peptide bond. Apart from the required knowledge of the correlation time, no calibration of a Karplus-type curve [for example $^3J(H_\alpha,N)$ (*16*)] is required for the measurement of the intervector angle.

The cross-correlated relaxation can be directly measured in double-quantum or zero-quantum coherence that is formed by either of the two spins out of the two pairs of nuclei (Fig. 3). In contrast to torsional angles that can be measured by scalar couplings about two or three bonds, the two internuclear vectors can in principle be separated by an arbitrary number of bonds in the molecule. However, double-quantum coherence needs to be excited and refocused between the nuclear spin states involved, which imposes some practical limitations on the distance between the internuclear vectors.

We demonstrated the measurement of this new parameter on the thrombin inhibitor rhodniin (a protein of 11-kD molecular mass) and measured the angle between the N_{k+1}-H^N_{k+1} and the $C_{\alpha,k}$-$H_{\alpha,k}$ vector (Fig. 3). Double-quantum coherence between the N_{k+1} and the $C_{\alpha,k}$ was excited in an HN(CO)CA (*17*)-derived experiment (Fig. 4). Evolution of this coherence in a constant time manner without proton decoupling during t_1 yields the expected four-line pattern from which the cross-correlated relaxation rates can be calculated according to Eq. 2. Figure 5 contains the double-quantum spectra of five representative amino acid residues of rhodniin (*18*, *19*) ex-

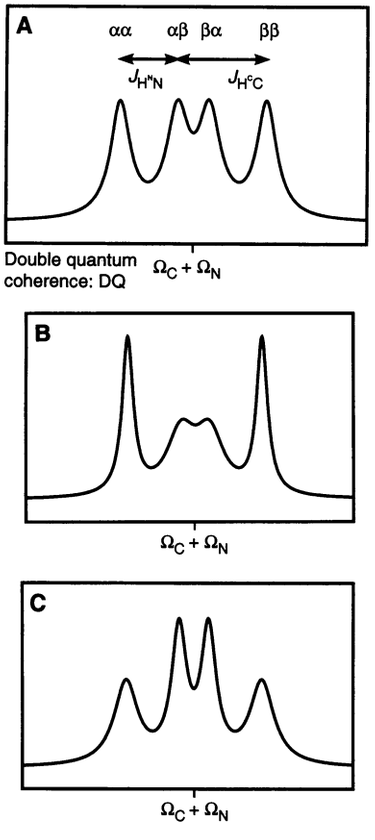

Fig. 2. Qualitative representation of the measured effect. The signal in the double-quantum (DQ) dimension is split due to the $^1J_{HN}$ and the $^1J_{CH}$ coupling. αα, αβ, βα, and ββ denote the four polarization states the two protons H_α and H^N can assume. The splitting of the signal without considering dipole-dipole cross-correlated relaxation is indicated in (**A**). For (**B**) and (**C**), θ was assumed to be 90° and 0°, respectively.

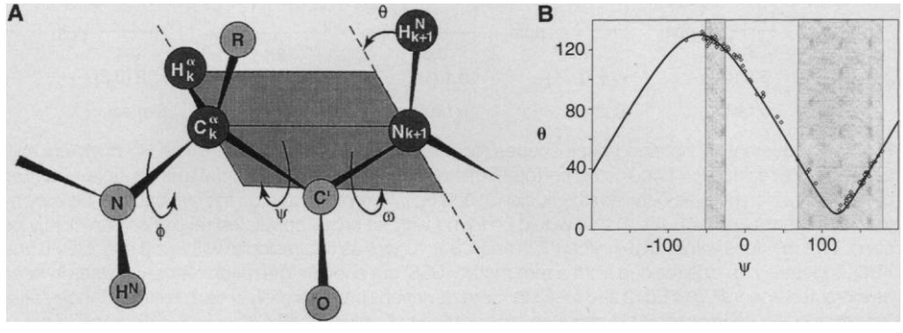

Fig. 3. (**A**) Schematic representation of the peptide backbone. The measured angle θ together with the N-H^N and C_α-H vectors is highlighted. (**B**) Theoretical and experimental correlation between θ and ψ is depicted, assuming planar peptide bond geometry. The exact equation is given in the text. Values found in a typical protein are indicated by squared boxes. The most populated regions are the α-helical region ($\psi = -39.8° \pm 12.2°$) and the β-sheet region ($\psi = 123.0° \pm 60.0°$) (*26*).

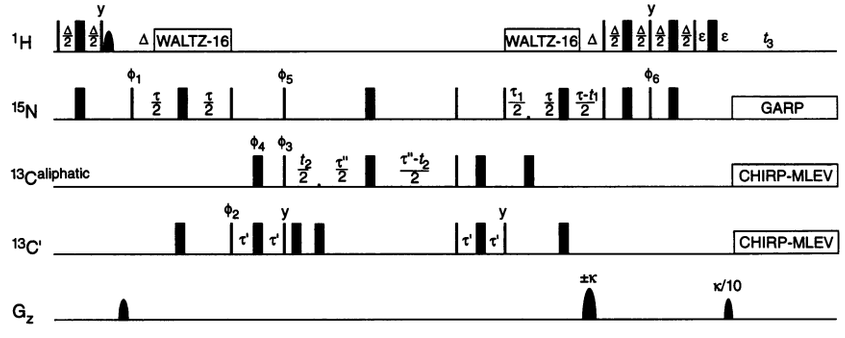

Fig. 4. NMR pulse sequence used for the measurement of the projection angles between the N-H^N and C_α-H_α vectors. Thin bars and thick bars represent 90° and 180° pulses. Default phases are x. Double and zero quantum coherence between N and C_α evolves during t_2. Δ = 5 ms, τ = 35 ms, $2\tau' = 9$ ms, $\tau'' = 26$ ms, and ε = 1.2 ms. Selective 90° and 180° pulses were applied on $C^{aliphatic}$ and C′ as G4 and G3 pulses (*27*). ϕ_1 = x, −x; ϕ_2 = 2(x), 2(−x); ϕ_3 = 4(x),4(−x); ϕ_5 = 8(x), 8(−x); $\phi_{rec} = \phi_1 + \phi_2 + \phi_3 + \phi_5$. Quadrature detection in the t_2 dimension is obtained by altering the phases ϕ_3 and ϕ_4 in the States-TPPI manner. Echo/anti-echo selection during t_1 is done by inversion of phase ϕ_6 = y, −y and of the second gradient. ϕ_3 and ϕ_5 are shifted by 90° for subsequent free induction decays (FIDs) and stored separately to differentiate between double and zero quantum coherence during t_2. Coaddition and subtraction of the FIDs yields the zero- and double-quantum spectrum, respectively. Broadband decoupling of aliphatic and carbonyl carbon resonances during the acquisition was achieved using MLEV expanded CHIRP pulses (*28*).

tracted from the two-dimensional experiment. The extracted relaxation rates $\Gamma^c_{i,j}$ with their standard deviation are given on the bottom of the plot for the selected peaks. Furthermore, the secondary structure element (SSE), which is found in the NMR structure for the respective residue, is cited. The experimental (from the three-dimensional experiment) and simulated (*20*) relaxation rates (for three correlation times τ_c = 5.0, 6.0, and 7.0 ns) are drawn in Fig. 6 as a function of the backbone angle ψ. The extracted cross-correlated relaxation times agree very well with the ψ angles found in the NMR structure.

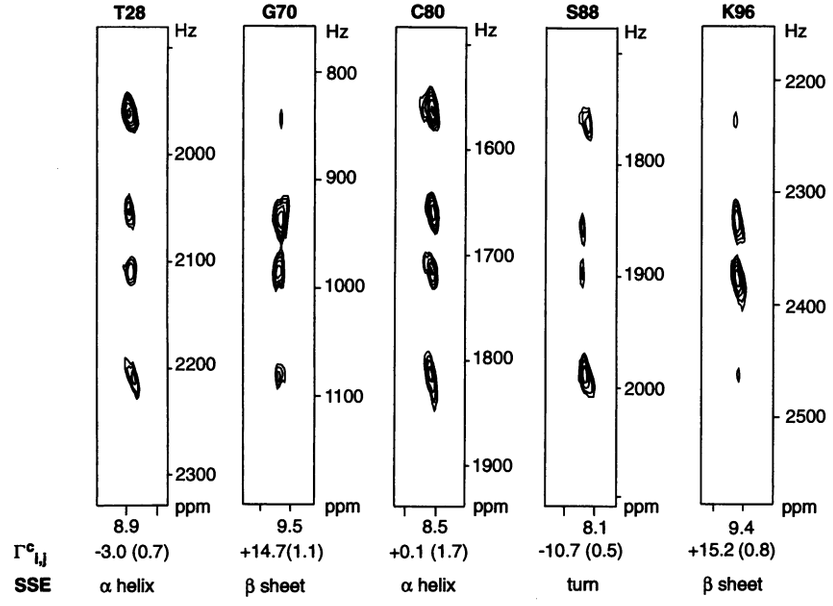

Fig. 5. Experimentally obtained peak shapes for selected residues in rhodniin. The H^N chemical shift (600 MHz) of residue k+1 (indicated on top of planes) is given on the horizontal axis. Double-quantum coherence which evolves between the nuclei C^α_k and N_{k+1} is represented on the vertical axis. Deviations from the intensity ratio (1:1:1:1) that would be found without cross-correlated relaxation can clearly be seen. Two residues within an α-helical (T28 and C80), as well as two residues within a β sheet (G70 and K96), together with one residue from a turn motive (S88) are shown. The mean relaxation rates in hertz as extracted according to Eq. 2 and their standard deviations are given below each residue. Single-letter abbreviations for the amino acid residues are as follows: C, Cys; G, Gly; K, Lys; S, Ser; and T, Thr.

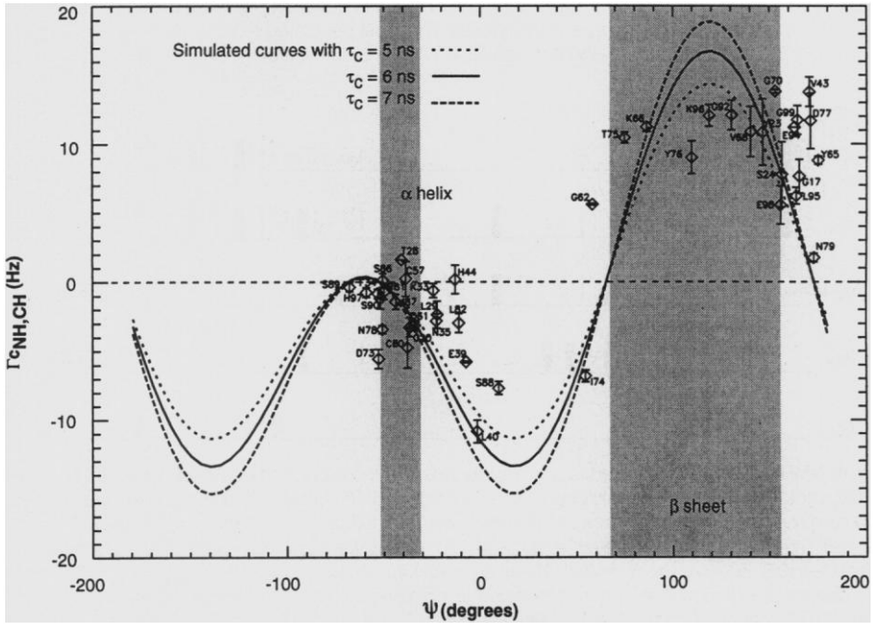

Fig. 6. Experimental and simulated relaxation rates $\Gamma^c_{i,j}$ in Hz due to cross-correlated relaxation as a function of the backbone angle ψ and three overall correlation times τ_c = 5.0, 6.0, and 7.0 ns. The ψ values for the selected residues are derived from the NMR structure of rhodniin that has been calculated with NOE data and torsional angle restraints. The range of ψ values found in α helices and β sheets are shaded in gray.

The methodology can be applied for all so-called "out and back" NMR experiments that are used for the assignment of proteins and oligonucleotides. The limitations with respect to size are the same as for these assignment experiments, because the proposed methodology relies exclusively on scalar couplings via one bond that are the biggest intramolecular interactions known for molecules in isotropic solutions. Long-range structural information is available if two nuclei can be correlated in an efficient way which can be achieved most efficiently for large deuterated proteins in which the H^N,H^N-NOE can be used for coherence transfer.

The proposed method yields different information from recently proposed measurement of residual dipolar couplings (*21*) and evaluation of ^{15}N-relaxation rates in anisotropically tumbling molecules (*22*). The residual dipolar couplings provide projection information of bond vectors on anisotropy tensors of the magnetic susceptibility. Relaxation rates yield projection information of bond vectors on tensors that describe the anistropy of the diffusive reorientation of the molecule. Thus, they provide indirect information about the relative orientation of interatomic vectors with respect to each other. By contrast, the proposed method yields direct information about bond vector projections provided double or zero quantum coherence can be excited between them. The cross-correlated relaxation rate is related to the interbond angle θ in an ambiguous way because of the $(3\cos^2\theta - 1)/2$ relationship (Eq. 3). However, this is also found for *J*-coupling constants, residual dipolar couplings, and projection on anisotropic reorientational tensors. The methodology can be extended to cross-correlation between dipolar couplings and CSA tensors of nitrogen (*23*, *24*) and C_α carbon (*23*, *25*), which can potentially be used to resolve the ambiguities of the $\Gamma^c_{i,j}$ (ψ) relation. The new spectroscopic parameter is uniquely powerful when a new set of NMR active nuclei is investigated in an organic molecule, for example, where neither the correlation time needs to be determined nor the interatomic distances need to be known, as $\Gamma^c_{i,j}$ changes sign at ±54° and ±126°. Fluctuations of θ that are on a time scale longer than τ_c lead to

averaging of the cross-correlated relaxation rate which may reveal slow motion up to 1 ms.

REFERENCES AND NOTES

1. K. Wüthrich, *NMR of Proteins and Nucleic Acids* (Wiley, New York, 1986).
2. I. Solomon, *Phys. Rev.* **99**, 559 (1955); ——— and N. Bloembergen, *J. Chem. Phys.* **25**, 261 (1956).
3. M. Karplus, *J. Chem. Phys.* **30**, 11 (1959); *J. Am. Chem. Soc.* **85**, 2870 (1963).
4. C. Griesinger, O. W. Sørensen, R. R. Ernst, *J. Magn. Reson.* **73**, 574 (1987); *J. Am. Chem. Soc.* **109**, 7227 (1987); H. Oschkinat *et al.*, *Nature* **332**, 374 (1988); M. Ikura, L. E. Kay, A. Bax, *Biochemistry* **29**, 4659 (1990); L. E. Kay, G. M. Clore, A. Bax, A. M. Gronenborn, *Science* **249**, 411 (1990); M. Ikura, A. Bax, G. M. Clore, A. M. Gronenborn, *J. Am. Chem. Soc.* **112**, 9020 (1990); G. M. Clore, L. E. Kay, A. Bax, A. M. Gronenborn, *Biochemistry* **30**, 12 (1991); E. R. P. Zuiderweg, A. M. Petros, S. W. Fesik, E. T. Olejniczak, *J. Am. Chem. Soc.* **113**, 370 (1991); G. M. Clore and A. M. Gronenborn, *Science* **252**, 1390 (1991).
5. B. H. Oh, W. M. Westler, P. Darba, J. L. Markley, *Science* **240**, 908 (1988); E. P Nikonowicz *et al.*, *Nucleic Acids Res.* **20**, 4507 (1992); R. T. Batey, M. Inada, E. Kujawinski, J. D. Puglisi, J. R. Williamson, *ibid.*, p. 4515; M. J. Michnicka, J. W. Harper, G. C. King, *Biochemistry* **32**, 395 (1993); S. Quant *et al.*, *Tetrahedron Lett.* **36**, 6649 (1994).
6. R. Brüschweiler, C. Griesinger, R. R. Ernst, *J. Am. Chem. Soc.* **111**, 8034 (1989).
7. M. Linder, A. Höhener, R. R. Ernst, *J. Chem. Phys.* **73**, 4959 (1980).
8. K. Schmidt-Rohr, *J. Am. Chem. Soc.* **118**, 7601 (1996); ———, *Macromolecules* **29**, 3975 (1996).
9. X. Feng, Y. K. Lee, D. Sandstroem, M. Eden, A. Sebald, M. H. Levitt, *Chem. Phys. Lett.* **257**, 314 (1996); G. Dabbagh, D. P. Weliky, R. Tycko, *ibid.* **27**, 6183 (1994).
10. N. Bloembergen, E. M. Purcell, R. V. Pound, *Phys. Rev.* **73**, 679 (1948).
11. L. G. Werbelow and D. M. Grant, *Adv. Magn. Reson.* **9**, 189 (1974).
12. A. Abragam, *The Principles of Nuclear Magnetism* (Clarendon Press, Oxford, 1961).
13. J. Cavanagh, W. J. Fairbrother, A. G. Palmer III, N. J. Skelton; *Protein NMR Spectroscopy* (Academic Press, San Diego, 1996).
14. L. E. Kay, D. A. Torchia, A. Bax, *Biochemistry* **28**, 8972 (1989); G. M. Clore, P. C. Driscoll, P. T. Wingfield, A. Gronenborn, *ibid.* **29**, 7378 (1990).
15. G. Lipari and A. J. Szabo, *J. Am. Chem. Soc.* **104**, 4546 (1982); N. Tjandra, A. Szabo, A. Bax, *ibid.* **118**, 6986 (1996); D. E. Woessner, *J. Chem. Phys.* **36**, 1 (1962); *ibid.* **37**, 647 (1962); G. Barbato, M. Ikura, L. E. Kay, R. W. Pasto, A. Bax, *Biochemistry* **31**, 5269 (1992); I. Q. H. Phan, J. Boyd, I. D. Campbell, *J. Biomol. NMR* **8**, 369 (1996).
16. A. C. Wang and A. Bax, *J. Am. Chem. Soc.* **117**, 1810 (1995).
17. A. Bax and M. Ikura, *J. Biomol. NMR* **1**, 99 (1991).
18. A. v. d. Locht *et al.*, *EMBO J.* **14**, 5149 (1995).
19. M. Maurer, V. Bellinger, T. Naumann, A. Diener, C. Griesinger, in preparation.
20. Z. Madi and R. R. Ernst, WTEST program package, Eidgenössische Technische Hochschule Zürich, Switzerland, 1989.
21. J. R. Tolman, J. M. Flanagan, M. A. Kennedy, J. H. Prestegaard, *Proc. Natl. Acad. Sci. U.S.A.* **92**, 9279 (1995); N. Tjandra, S. Grzesiek, A. Bax, *J. Am. Chem. Soc.* **118**, 6264 (1996).
22. N. Tjandra, H. Kuboniwa, H. Ren, A. Bax, *Eur. J. Biochem.* **230**, 1014 (1995).
23. T. M. Duncan, *A Compilation of Chemical Shift Anisotropies* (Farragut Press, Chicago, 1990).
24. M. D. Lumsden *et al.*, *J. Am. Chem. Soc.* **116**, 1403 (1994); C. J. Hartzell, M. Whitfield, T. G. Oas, G. P. Drobny, *ibid.* **109**, 5966 (1987).
25. N. Janes, S. Ganapathy, E. Oldfield, *J. Magn. Reson.* **54**, 111 (1983).
26. L. J. Smith *et al.*, *J. Mol. Biol.* **255**, 494 (1996).
27. L. Emsley and G. Bodenhausen, *J. Magn. Reson.* **82**, 211 (1989); *Chem. Phys. Lett.* **165**, 469 (1989).
28. R. Fu and G. Bodenhausen, *Chem. Phys. Lett.* **245**, 415 (1995).

29. Supported by the Fonds der Chemischen Industrie and in part by the DFG under grant 1211/6-1. M.H. acknowledges a Ph.D. fellowship by the Fonds der Chemischen Industrie. We thank M. Maurer for providing the assignments and the NMR structural data of rhodniin in solution. We are grateful for continuous support by T. Keller and W. Bermel, Bruker, Karlsruhe, Germany.

10 December 1996; accepted 14 March 1997

Large Molecular Third-Order Optical Nonlinearities in Polarized Carotenoids

Seth R. Marder,* William E. Torruellas,† Mirelle Blanchard-Desce, Vincent Ricci, George I. Stegeman, Sharon Gilmour, Jean-Luc Brédas, Jun Li, Greg U. Bublitz, Steve G. Boxer

Garito and co-workers have suggested a mechanism to dramatically increase the second hyperpolarizability, γ, in linear π-electron–conjugated molecules. Polarization is introduced that leads to a difference between the dipole moments of the molecule's ground state and excited state. Here a series of carotenoids was examined that had increasing intramolecular charge transfer (ICT) from the polyenic chain to the acceptor moiety in the ground state, and γ was measured for these compounds as a function of wavelength by third-harmonic generation. The compound with the greatest ICT exhibited a 35-fold enhancement of γ_{max} (the γ measured at the peak of the three-photon resonance) relative to the symmetric molecule β-carotene, which itself has one of the largest third-order nonlinearities known. Stark spectroscopic measurements revealed the existence of a large difference dipole moment, $\Delta\mu$, between the ground and excited state. Quantum-chemical calculations underline the importance of interactions involving states with large $\Delta\mu$.

Molecules with large third-order optical nonlinearities (characterized by large second hyperpolarizabilities, γ) are required for photonic applications including all-optical switching, data processing, and eye and sensor protection. In contrast to second-order nonlinear materials, for which the basic structure-property relations are both relatively well understood and well explored, for third-order materials a comparable level of understanding is only just emerging. Garito and co-workers have suggested a mechanism to dramatically increase γ (*1*, *2*), and they calculated that polarized polyenes could have very large γ, relative to unsubstituted polyenes of comparable length, because of symmetry breaking. A parallel situation exists in semiconductor quantum wells where asymmetrization has led to some of the largest second- and third-order nonlinearities ever observed in the mid- to far-infrared portion of the spectrum, both with and without the presence of permanent dc fields (*3*–*5*). The results of recent computational and experimental studies on small model systems agree with the predictions of Garito *et al.* (*6*–*9*). Nonetheless, molecules that exhibit extremely large γ according to the mechanism predicted by Garito *et al.* are still quite unusual (*10*–*12*). Indeed, γ values are still, perhaps with rare exceptions (*13*), not sufficiently large for realistic applications to ultrafast information-processing optical devices. Here we explored the hypothesis of Garito *et al.* further and found that large enhancements in γ can be achieved in a variety of acceptor-substituted carotenoids as determined by wavelength-dependent third-harmonic generation experiments (THG).

Several groups have shown from a sum-over-states analysis of γ derived from perturbation theory that three classes of terms

S. R. Marder, Beckman Institute, California Institute of Technology, Pasadena, CA 91125, USA, and Jet Propulsion Laboratory, California Institute of Technology, Pasadena, CA 91109, USA.
W. E. Torruellas, V. Ricci, G. I. Stegeman, Center for Research on Education, Optics, and Lasers, University of Central Florida, 4000 Central Florida Boulevard, Orlando, FL 32816, USA.
M. Blanchard-Desce, Ecole Normale Supérieure, Département de Chimie (Unité de Recherche Associée 1679 CNRS), 24 rue Lhomond 75231, Paris Cedex 05, France.
S. Gilmour, Jet Propulsion Laboratory, California Institute of Technology, Pasadena, CA 91109, USA.
J.-L. Brédas and J. Li, Center for Research on Molecular Electronics and Photonics, Université de Mons-Hainaut, Place du Parc 20, B-7000 Mons, Belgium.
G. U. Bublitz and S. G. Boxer, Department of Chemistry, Stanford University, Stanford, CA, 94305, USA.

*To whom correspondence should be addressed.
†Present address: Department of Physics, Washington State University, Pullman, WA 99164, USA.